J|A|C|S ARTICLES

Published on Web 04/30/2009

Spin Trapping of Au−H Intermediate in the Alcohol Oxidation by Supported and Unsupported Gold Catalysts

Marco Conte,[†] Hiroyuki Miyamura,[‡] Shū Kobayashi,[‡] and Victor Chechik*[,†]

Department of Chemistry, University of York, Heslington, York, YO10 5DD, United Kingdom, and Graduate School of Pharmaceutical Sciences, The University of Tokyo, Hongo, Bunkyo-ku, Tokyo, 113-0033, Japan

Received December 18, 2008; E-mail: vc4@york.ac.uk

Abstract: Electron paramagnetic resonance (EPR) spectroscopy and spin trapping were used to explore the mechanism of alcohol oxidation over gold catalysts. Reaction of secondary alcohols with supported and unsupported gold catalysts (e.g., Au/CeO_2, polymer-incarcerated Au nanoparticles, PPh_3-protected Au nanoparticles) in the presence of spin traps led to the formation of a hydrogen spin adduct. Using isotope labeling, we confirmed that the hydrogen in the spin adduct originates from the cleavage of the C−H bond in the alcohol molecule. The formation of the hydrogen spin adduct most likely results from the abstraction of hydrogen from the Au surface by a spin trap. These results thus strongly suggest intermediate formation of Au−H species during alcohol oxidation. The role of oxygen in this mechanism is to restore the catalytic activity rather than oxidize alcohol. This was further confirmed by carrying out gold-catalyzed alcohol oxidation in the absence of oxygen, with nitroxides as hydrogen abstractors. The support (e.g., metal oxides) can activate oxygen and act as an H abstractor from the gold surface and hence lead to a faster recovery of the activity. Peroxyl radicals were also observed during alcohol oxidation, consistent with a free-radical autoxidation mechanism. However, this mechanism is likely to be a minor side reaction, which does not lead to the formation of an appreciable amount of oxidation products.

1. Introduction

Alcohol oxidation is one of the most industrially important reactions,[1−3] and one that gold based catalysts carry out most efficiently.[4−6] However, despite a number of promising high impact applications, mechanistic aspects of gold catalysis are not well understood. In particular, gold activity in alcohol oxidation in the absence of base,[7] the nature of C−H bond activation,[8,9] and the role of superoxide species in the case of supported catalysts[10] need further investigation. Clarification of the reaction mechanism is crucial for future design of catalysts with enhanced performance.

As well as gold, many metal nanoparticle based catalysts such as palladium,[11,12] platinum,[13,14] ruthenium,[15] and silver[16] are able to oxidize alcohols to ketones. In the case of palladium and platinum, the reaction mechanism (consistent with the observed activity pattern) is believed to include sequential cleavage of O−H and C−H bonds to give a ketone and two hydrogen atoms adsorbed over the metal surface, which can be oxidized by oxygen to give water.[17,18] The mechanism of alcohol oxidation by ruthenium complexes involves oxidative dehydrogenation with the role of oxygen limited to the restoration of the catalyst oxidation state.[19] With silver nanoparticles, oxidative dehydrogenation is also operating, but in this case prior activation of molecular oxygen is required.[20] Very recently, Corma and co-workers proposed a β-hydride shift from alcohol to form a Au−H intermediate as a key step of aerobic alcohol

[†] University of York.
[‡] The University of Tokyo.

(1) Speight, J. G. *Chemical and Process Design Handbook*; McGraw-Hill: New York, 2002.
(2) McKetta, J. *Chemical Processing Handbook*; Marcel Dekker: New York, 1994.
(3) Mallat, T.; Baiker, A. *Chem. Rev.* **2004**, *104*, 3037–3058.
(4) Enache, D. I.; Edwards, J. J.; Landon, P.; Solsona-Espriu, B.; Carley, A. F.; Herzing, A. A.; Watanabe, M.; Kiely, C. J.; Knight, D. W.; Hutchings, G. J. *Science* **2006**, *311*, 362–365.
(5) Abad, A.; Almela, C.; Corma, A.; García, H. *Chem. Commun.* **2006**, 3178–3180.
(6) Della Pina, C.; Falletta, E.; Prati, L.; Rossi, M. *Chem. Soc. Rev.* **2008**, *37*, 2077–2095.
(7) Taarning, E.; Madsen, A. T.; Marchetti, J. M.; Egeblad, K.; Christensen, C. H. *Green Chem.* **2008**, *10*, 408–414.
(8) Arcadi, A. *Chem. Rev.* **2008**, *108*, 3266–3325.
(9) Li, Z.; Brouwer, C.; He, C. *Chem. Rev.* **2008**, *108*, 3239–3265.
(10) Fierro-Gonzalez, J. C.; Bhirud, A. A.; Gates, B. C. *Chem. Commun.* **2005**, 5275–5277.
(11) Mori, K.; Hara, T.; Mizugaki, T.; Ebitani, K.; Kaneda, K. *J. Am. Chem. Soc.* **2004**, *126*, 10657–10666.
(12) Schuurman, Y.; Kuster, B. F. M.; van der Wiele, K.; Marin, G. B. *Appl. Catal. A* **1992**, *89*, 31–46.
(13) Keresszegi, C.; Mallat, T.; Grunwaldt, J.-D.; Baiker, A. *J. Catal.* **2004**, *225*, 138–146.
(14) Korovchenko, P.; Donze, C.; Gallezot, P.; Besson, M. *Catal. Today* **2007**, *121*, 13–21.
(15) Takezawa, E.; Sakaguchi, S.; Ishii, Y. *Org. Lett.* **1999**, *1*, 713–715.
(16) Vodyankina, O. V.; Kurina, L. N.; Boronin, A. I.; Salanov, A. N. *Stud. Surf. Sci. Catal.* **2000**, *130*, 1775–1781.
(17) Di Cosimo, R.; Whitesides, G. M. *J. Phys. Chem.* **1989**, *93*, 768–775.
(18) Vinke, P.; van Dam, H. E.; van Bekkum, H. *Stud. Surf. Sci. Catal.* **1990**, *55*, 147–157.
(19) Kaneda, K.; Yamaguchi, K.; Mori, K.; Mizugaki, T.; Ebitani, K. *Catal. Surv. Jpn.* **2000**, *4*, 31–38.
(20) Yang, Z.; Li, J.; Yang, X.; Xie, X.; Wu, Y. *J. Mol. Catal. A: Chem.* **2005**, *241*, 15–22.

oxidation by supported gold nanoparticles.[21] This has been supported by Christensen and co-workers[22] using Hammett plots[23] for a series of para-substituted benzyl alcohols.

Hydride species over a metal surface have been detected for Pd and Pt.[11,24] In contrast, the existence of Au−H species has only been proposed for homogeneous catalysis, e.g., in the formation of alkene complexes by β-elimination from Au^{3+} alkyl complexes,[25] in the catalyzed enantioselective hydrogenation of alkenes and imines by Au complexes,[26] and in addition reactions of 1,3-diketones to alkenes.[27] However, direct evidence of Au−H species has proved elusive with the exception of an *in situ* FT-IR study of adsorbed isopropanol over Au/CeO_2.[28] The latter method provided evidence for Au−H formation only at low pressures and could not be applied to liquid phase systems.

This prompted us to carry out a mechanistic study involving both supported and unsupported catalysts to identify the common factors that govern gold activity, particularly in the absence of base and under realistic reaction conditions. Addition of base significantly improves the efficiency of alcohol oxidation for many gold based catalysts;[29,30] however this can also lead to side reactions and hence diminished selectivity.[31] Some gold catalysts can perform efficient alcohol oxidation in the absence of base, particularly in the presence of palladium metal.[32,33] We explored mechanistic features of three different types of Au catalysts: Au nanoparticles supported on ceria (Au/CeO_2),[34] polymer-incarcerated Au nanoparticles (Au-PI, the polymer is based on polystyrene, details are in the Supporting Information),[35] and soluble triphenylphosphine-protected Au nanoparticles ($AuPPh_3$).[36] This choice covers metal oxide supported, "naked" polymer supported,[37−39] and unsupported soluble nanoparticles. While both Au/CeO_2 and Au-PI catalysts can efficiently oxidize alcohols, $AuPPh_3$ shows very little bulk conversion.

To test if the alcohol oxidation proceeds *via* a radical mechanism, we employed EPR spectroscopy and a spin trapping technique.[40−42] Spin trapping relies on fast selective addition (trapping) of short-lived radicals to a diamagnetic spin trap, usually a nitrone or a nitroso compound. The product of this addition (spin adduct) is a persistent free radical (nitroxide) with a sufficiently long lifetime to enable detection by conventional EPR spectroscopy. Magnetic properties of the spin adduct often make it possible to assign the structure of the original short-lived radicals. Apart from reactions with free radicals, spin traps are also capable of abstracting intermediates adsorbed over metal surfaces, often giving the same paramagnetic spin adducts.[43,44] Structures of spin traps used in this study are shown in Scheme 1.

Scheme 1. Chemical Structures of DMPO and PBN Spin Traps and Trapping of a Free Radical (a) and Adsorbed Species over Surface (b)

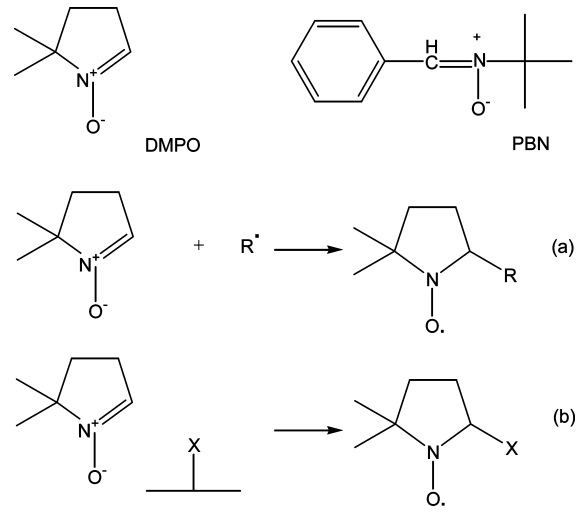

2. Results and Discussion

2.1. Formation of an H Spin Adduct during Alcohol Oxidation. A reaction of $AuPPh_3$ nanoparticles with a degassed sample of 2-pentanol in toluene in the presence of DMPO at room temperature produced a persistent free radical which was identified from the EPR spectra as a DMPO-H adduct by comparison with the literature[45] (Figure 1a, $a_N = 14.98$, $a_{H(1)} = a_{H(2)} = 19.83$ G). When Au/CeO_2 was used with 3-octanol in toluene at 70 °C, an identical strong spectrum of DMPO-H adduct was observed (Figure 1b). The structure assignment was also confirmed by comparison with the EPR spectra of an authentic DMPO-H spin adduct prepared by reaction of PbO_2 with $NaBH_4$ (Figure S1).[46] The interpretation of EPR spectra was further supported by analysis of the time-dependent evolution of DMPO-H signal which confirmed the presence of only one type of radical in the reaction mixture (Figure S2). When Au-PI and PBN as a spin trap were used with 1-phenylethanol in toluene at 70 °C, a PBN-H adduct was observed[47] (Figure 1c, $a_N = 15.39$, $a_{H(1)} = a_{H(2)} = 7.99$ G).

(21) Abad, A.; Corma, A.; García, H. *Chem. Eur. J.* **2008**, *14*, 212–222.
(22) Fristrup, P.; Johansen, L. B.; Christensen, C. H. *Catal. Lett.* **2008**, *120*, 184–190.
(23) Hansch, C.; Leo, A.; Taft, R. W. *Chem. Rev.* **1991**, *91*, 165–195.
(24) Keresszegi, C.; Mallat, T.; Grunwaldt, J.-D.; Baiker, A. *J. Catal.* **2004**, *225*, 138–146.
(25) Bond, G. C.; Louis, C.; Thompson, D. T. *Catalysis by gold*; Catalytic Science Series; Imperial College Press: London, 2006; Vol. 6.
(26) González-Arellano, C.; Corma, A.; Iglesias, M.; Sánchez, F. *Chem. Commun.* **2005**, 3451–3453.
(27) Yao, X.; Li, C.-J. *J. Am. Chem. Soc.* **2004**, *126*, 6884–6885.
(28) Abad, A.; Concepción, P.; Corma, A.; García, H. *Angew. Chem.* **2005**, *117*, 4134–4137.
(29) Miyamura, H.; Matsubara, R.; Kobayashi, S. *Chem. Commun.* **2008**, 2031–2033.
(30) Prati, L.; Rossi, M. *J. Catal.* **1998**, *176*, 552–560.
(31) Besson, M.; Gallezot, P. *Catal. Today* **2000**, *57*, 127–141.
(32) Corma, A.; Garcia, H. *Chem. Soc. Rev.* **2008**, *37*, 2096–2126.
(33) Hutchings, G. J. *Chem. Commun.* **2008**, 1148–1164.
(34) Corma, A.; Domine, M. E. *Chem. Commun.* **2005**, 4042–4044.
(35) Miyamura, H.; Matsubara, R.; Miyazaki, Y.; Kobayashi, S. *Angew. Chem., Int. Ed.* **2007**, *46*, 4151–4154.
(36) Ionita, P.; Conte, M.; Gilbert, B. C.; Chechik, V. *Org. Biomol. Chem.* **2007**, *5*, 3504–3509.
(37) Akiyama, R.; Kobayashi, S. *J. Am. Chem. Soc.* **2003**, *125*, 3412–3413.
(38) Okamoto, K.; Akiyama, R.; Yoshida, H.; Yoshida, T.; Kobayashi, S. *J. Am. Chem. Soc.* **2005**, *127*, 2125–2135.
(39) Kobayashi, S.; Miyamura, H.; Akiyama, R.; Ishida, T. *J. Am. Chem. Soc.* **2005**, *127*, 9251–9254.
(40) Claus, P.; Brückner, A.; Mohr, C.; Hofmeister, H. *J. Am. Chem. Soc.* **2000**, *122*, 11430–11439.
(41) Rajh, T. V.; Poluektov, O.; Dubinski, A. A.; Wiederrecht, G.; Thurnauer, M.; Trifunac, A. D. *Chem. Phys. Lett.* **2001**, *344*, 31–39.
(42) Ionita, P.; Volkov, A.; Jeschke, G.; Chechik, V. *Anal. Chem.* **2008**, *80*, 95–106.
(43) Burt, A.; Emery, M.; Maher, J.; Mile, B. *Magn. Reson. Chem.* **2001**, *39*, 85–88.
(44) Carley, A. F.; Edwards, H. A.; Mile, B. M.; Roberts, W.; Rowlands, C. C.; Hancock, F. E.; David Jackson, S. *J. Chem. Soc., Faraday Trans.* **1994**, *90*, 3341–3346.
(45) Maillard, P.; Massot, J. C.; Giannotto, C. *J. Organomet. Chem.* **1978**, *159*, 219–227.
(46) Ionita, P.; Gilbert, B. C.; Chechik, V. *Angew. Chem., Int. Ed.* **2005**, *117*, 3786–3788.

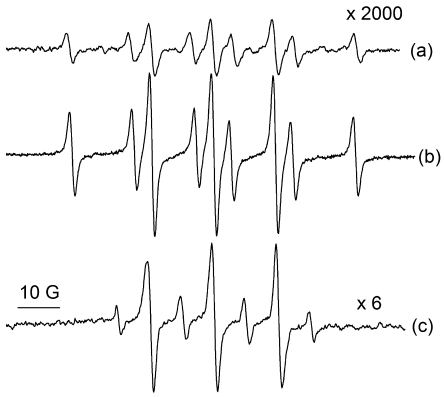

Figure 1. EPR spectra of H spin adducts formed during aerobic oxidation of secondary alcohols over supported and unsupported gold catalysts: (a) DMPO-H adduct for $AuPPh_3$ nanoparticles and 2-pentanol, (b) DMPO-H adduct for Au/CeO_2 and 3-octanol and (c) PBN-H adduct for Au-PI and 1-phenylethanol.

The spin trapping technique is known to be prone to artifacts. Apart from the radical addition to the spin trap, spin adducts could also be formed by nucleophilic addition followed by oxidation, or by oxidation of the spin trap followed by nucleophilic addition. For instance, one can envisage a hydride transfer from the alcohol molecule to the spin trap leading to an H spin adduct after oxidation of the intermediate hydroxylamine. Such nucleophilic addition artifacts will be facilitated in the presence of base. However, control experiments showed that no H adduct is formed in the absence of alcohol or catalyst. In the presence of strong base, artifacts were indeed observed; however no H spin adduct was detected even in this case (Figure S3). This suggests that the observed H spin adduct cannot be formed *via* hydride transfer from alcohol to the spin trap followed by oxidation. We should stress that all results presented in this work were obtained in the absence of base.

Analysis of bulk reaction mixtures by ^1H and ^{13}C NMR showed that the only products of alcohol oxidation are the corresponding ketone and water, and ketone is formed stoichiometrically from the alcohol (full details in supplementary data, Figures S4−S8). Integration of ^1H NMR spectra showed that one molecule of water was formed for every molecule of alcohol oxidized. Under reaction conditions used for the EPR experiments, the conversion of alcohols to ketones varied for different catalysts. The reaction of $AuPPh_3$ with alcohols gave only a trace amount of ketone (*ca.* 0.4% at room temperature). This catalyst showed no turnover and is therefore not suitable for synthetic applications. Oxidation of 1-phenylethanol in toluene in the presence of Au-PI led to 25% conversion at 70 °C. This catalyst can perform much better in the presence of base; however, we avoided the use of base to reduce the possibility of artifacts (*vide supra*). When Au/CeO_2 was used for 3-octanol oxidation in toluene, a bulk conversion of 26% was achieved under the same spin trapping conditions, at 70 °C. The much higher EPR intensity of the H adduct for the active catalysts (Au-PI, Au/CeO_2) as compared to the inactive one ($AuPPh_3$) suggests that formation of the H adduct is involved in alcohol oxidation. The fact that the H spin adduct was observed in reactions of alcohols with all Au catalysts suggests a common reaction mechanism. This is an important conclusion as it implies that the mechanism of Au catalyzed alcohol oxidation does not depend on the properties of the support.

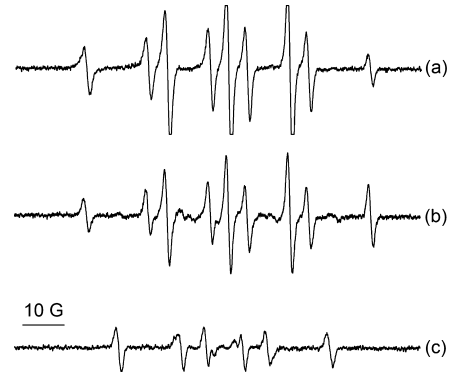

Figure 2. Spin adducts formed from DMPO in a reaction of Au/CeO_2 with $(CH_3)_2CHOH$ (a), $(CH_3)_2CHOD$ (b), and $(CD_3)_2CDOD$ (c).

The H spin adduct could have originated either from an OH or a CH group of the alcohol. To unambiguously determine the source of H atoms, we carried out an isotope labeling study. In Au/CeO_2-catalyzed oxidation of $(CH_3)_2CHOH$, $(CH_3)_2CHOD$ and $(CD_3)_2CDOD$, an identical DMPO-H spin adduct was detected for the two former substrates. The concentration of DMPO-H adduct in these reactions was the same within experimental error (*ca.* a factor of 2; see Experimental Section). The perdeuterated isopropanol gave no hydrogen adduct (judging from the signal-to-noise ratio, the maximum possible intensity of DMPO-H adduct in Figure 2c is at least 15 times lower than that in Figure 2a,b). A weaker adduct of the carbon-centered radical[48] (a_N = 14.90, a_H = 22.80 G) was instead detected (*vide infra*) (Figure 2c). A small amount of carbon-centered radicals can also be observed in Figure 2b.

These data suggested that the detected H spin adduct is due to C−H cleavage. The fact that the D spin adduct could not be detected under identical reaction conditions when a deuterated isopropanol was used as a substrate is only consistent with the primary kinetic isotope effect. Our conclusion that the H adducts originate from the C−H rather than O−H bond cleavage were unambiguously proven by the observation of a very weak DMPO-D adduct signal[49] (a_N = 13.86, a_H = 19.80, a_D = 2.99 G) (and no DMPO-H signal at all) in reactions of $(CD_3)_2CDOD$ and $(CD_3)_2CDOH$ with Au/CeO_2 (Figures S9 and S10) after additional deoxygenation of the sample prior to thermal treatment.

To independently assess the kinetic isotope effect, we monitored oxygen consumption in the oxidation of $(CH_3)_2CHOH$ and $(CD_3)_2CDOD$ using an EPR oximetry method (full details are in the Supporting Information, Figure S11). The ratio of oxygen decay rates k_H/k_D = 5 confirms the primary kinetic isotope effect. Additionally, the primary kinetic isotope effect was also confirmed by GC−MS analysis of the products formed during competitive oxidation of a 1:1 $(CH_3)_2CHOH$/$(CD_3)_2CDOD$ mixture (Supporting Information). We conclude therefore that the C−H bond cleavage is the rate-determining step in the alcohol oxidation. This is consistent with a recent report[21] on supported gold catalysis.

2.2. Origin of the H Spin Adduct. Observation of H spin adduct may have been explained by the formation of free hydrogen radicals during alcohol oxidation. For instance, H_2 is known to form in Pd/Pt catalyzed reactions if local concentration

(47) Janzen, E. G.; Kasai, T.; Kuwata, K. *Bull. Chem. Soc. Jpn.* **1973**, *46*, 2061–2062.
(48) Janzen, E. G.; Liu, J.-P. *J. Magn. Reson.* **1973**, *9*, 510–512.
(49) Maillard, P.; Giannotti, C. *Can. J. Chem.* **1982**, *60*, 1402–1413.

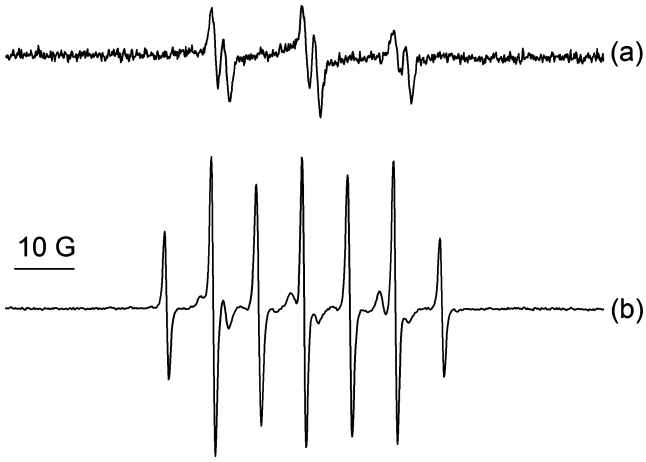

Figure 3. Spin adducts formed from DMPO in a reaction of Au/CeO_2 with 3-octanol in the presence of (a) poly-PBN (weak peroxyl radicals are observed) and (b) soluble PBN (a strong PBN-H adduct signal is detected).

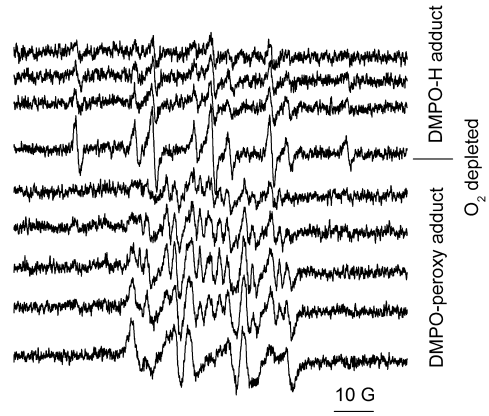

Figure 4. EPR spectra of Au/CeO_2 + 3-octanol + DMPO reaction mixture in a sealed system recorded without prior degassing. Spectra were recorded every 2.4 min.

of oxygen becomes very small.[50] In the presence of oxygen, free hydrogen atoms could be expected to form $HOO^{\bullet}$ and eventually H_2O as a final product, consistent with the experimental observations.[51] Formation of free $H^{\bullet}$ in the reaction mixtures, however, would have been a very unusual conclusion. In the absence of spin trapping artifacts as established by control experiments, the only viable alternative explanation for the H spin adduct formation is abstraction of hydrogen from the Au surface by the spin trap. The potential reaction of spin traps with the adsorbed species can never be ruled out with spin trapping over solid surfaces.[52]

To determine if the H atoms are free in solution or adsorbed on the Au surface, we explored spin trapping with a polymer-attached nitrone. The successful spin trapping of a variety of short-lived free radicals (e.g., carbon and oxygen centered)[53] with the immobilized spin trap suggested that if H atoms are formed in the solution, they will react with the immobilized spin trap. The immobilized trap, however, cannot scavenge hydrogen if it is bonded to a surface. Gold-catalyzed alcohol oxidation was thus tested with poly N-(*m*-vinylbenzylidene)-*tert*-butylamine N-oxide (poly-PBN), which was synthesized following a literature procedure[53] (full details in Supporting Information). In a control experiment, we showed that PBN and poly-PBN have nearly identical trapping efficiency for oxygen-centered free radicals in homogeneous media. In Au/CeO_2-catalyzed alcohol oxidation, however, the behavior of PBN and poly-PBN was different. A strong signal of PBN-H adduct ($a_N = 15.24$, $a_{H(1)} = a_{H(2)} = 7.77$ G) was detected with PBN, but no H-adduct was observed in case of the polymer based spin trap (Figure 3). In contrast, weak peroxyl adducts were detected (Figure 3a).[54] (coupling constants a_N=15.19 and a_H=1.76 G). Weak peroxyl adducts were also detected with PBN (Figure 3b).

These results strongly suggest that while small amount of peroxyl radicals is formed in solution (and is detected by both dissolved and immobilized spin traps), the observation of an H spin adduct is due to the abstraction of hydrogen from the Au surface by the spin trap. DMPO-H adduct could be formed by either abstraction of an H atom from Au−H, or abstraction of H^- from Au−H followed by oxidation. High intensity of the H adducts detected in the absence of oxygen suggest the abstraction of H atom rather then H^-; in either case, however, our data suggest formation of the Au−H species. We believe that this is the strongest available evidence for the existence of hydrogen atoms adsorbed over gold surface, and their involvement in alcohol oxidation reactions.

2.3. Role of Free Radicals in Alcohol Oxidation. The trapping of carbon and/or oxygen centered radicals in some alcohol oxidations (Figures 2, 3) prompted us to investigate the role of free radical intermediates in this reaction. All spin trapping experiments reported above were carried out in sealed, degassed samples. In the presence of air, no H spin adduct can be detected. Presumably, oxygen can abstract hydrogen atoms from the gold surface much faster than the spin trap, possibly *via* oxygen reduction reaction.[55] Abstraction of hydride ion from the Au surface by oxygen to form OOH^- also cannot be ruled out. Only after oxygen has been depleted or removed, the spin trap can act as a hydrogen abstractor. We found that when alcohol oxidation is carried out in a sealed system without prior degassing, peroxyl adducts are observed initially, with the detection of H adduct after all oxygen has been consumed (Figure 4).

The signals of peroxy spin adducts, however, are very weak and overlap with the hydrogen spin adduct signals. Hence, they cannot be unambiguously assigned to DMPO-OOH or DMPO-$OOC(OH)CR_2$. adducts, with the latter from a possible autoxidation pathway.[56] In order to detect these radicals without the overlapping DMPO-H adduct, we recorded EPR spectra of catalytic reactions using $(CD_3)_2CDOD$ as a substrate in a sealed system using Au/CeO_2 as a catalyst at 70 °C without prior degassing (Figure 5). Thanks to the primary kinetic isotope effect, the C-D bond cleavage in the deuterated substrate is suppressed, and peroxyl radicals dominate the EPR spectra. The radicals are present from the beginning of the reaction in this case, with the spectra becoming progressively sharper due to oxygen consumption in the sealed system.

(50) Kluytmans, J. H. J.; Markusse, A. P.; Kustera, B. F. M.; Marin, G. B.; Schouten, J. C. *Catal. Today* **2000**, *57*, 143–155.
(51) Besson, B.; Gallezot, P. *Catal. Today* **2000**, *57*, 127–141.
(52) Klabunde, K. J.; Nievest, I. *J. Phys. Chem.* **1988**, *92*, 2521–2525.
(53) Ren, J.; Sakakibara, K.; Hirota, M. *React. Polym.* **1994**, *22*, 107–114.
(54) Ohto, N.; Niki, E.; Kamiya, Y. *J. Chem. Soc., Perkin Trans. 2* **1977**, 1770.
(55) Zhang, J.; Sasaki, K.; Sutter, E.; Adzic, R. R. *Science* **2007**, *315*, 220–222.
(56) Sheldon R. A.; Kochi, J. K. *Metal-Catalyzed Oxidations of Organic Compounds*; Academic Press: New York, 1981.

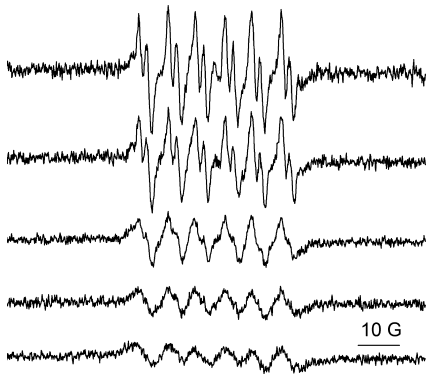

Figure 5. EPR spectra of Au/CeO_2 + $(CD_3)_2CDOD$ + DMPO reaction mixture recorded without prior degassing. Spectra were recorded each 30 min.

Simulation of the well-defined spectra in Figure 5, led to hyperfine values of $a_N = 13.48$, $a_{H(\beta)} = 7.07$, $a_{H(\gamma)} = 1.79$ G, which are very similar to the values obtained with 3-octanol in the beginning of the reaction ($a_N = 13.33$, $a_{H(\beta)} = 6.80$, $a_{H(\gamma)} = 1.83$ G, Figure 4). Small differences in the hyperfine values can be assigned to solvent effect. These hyperfine values are typical of DMPO-$OOCR_3$.[57] and not DMPO-OOH adducts which are expected to have $a_{H(\beta)}$ in the range of 11 G.[58] We conclude therefore that some carboperoxyl radicals are formed during Au-catalyzed alcohol oxidation. These radicals, however, are due to a minor side reaction, which likely does not yield appreciable amounts of products under these conditions. Carboperoxyl species are likely to results from an autoxidation process that under appropriate conditions can be productively used for the H_2O_2 manufacture.[33,56]

2.4. Oxidation with Nitroxides and the Role of Oxygen. An important question in the Au-catalyzed alcohol oxidation is if oxygen is needed to form the final product (ketone) or the role of oxygen is limited to regeneration of the catalytic activity by abstracting an H atom from the gold surface. To answer this question, 2,2′,6,6′-tetramethylpiperidine *N*-oxyl (TEMPO) was added to the Au-catalyzed reaction mixtures. TEMPO is a good hydrogen abstractor (it can abstract benzylic H atom[59] or an H atom from iron based complexes[60]), and we hoped that it could abstract a hydrogen atom from the Au surface during catalytic reactions carried out in the absence of oxygen. EPR spectra of TEMPO are also sensitive to oxygen concentration, and hence it can be used to monitor oxygen consumption in the sealed catalytic reaction mixture[61] *via* line sharpening. In addition, TEMPO itself can catalyze mild and selective oxidation of alcohols to aldehydes, ketones, and carboxylic acids[62] in the presence of a stoichiometric amount of sodium hypochlorite, sodium bromite, or sodium chlorite[63,64] (which are needed to generate oxoammonium salt as an active oxidant). However, this latter catalytic system is effective only with easily oxidizeable benzylic and allylic alcohols. To ensure that the background TEMPO-catalyzed alcohol oxidation does not compete with the Au catalyzed process, the most efficient catalyst (Au/CeO_2) was used. Under our conditions, the rate of TEMPO-catalyzed alcohol oxidation was at least 8 times slower than that of the Au-catalyzed reaction (full details in the Supporting Information, Figure S12). Therefore, the role of TEMPO in Au-catalyzed alcohol oxidation is twofold: to abstract hydrogen from the gold surface and report on the oxygen concentration.

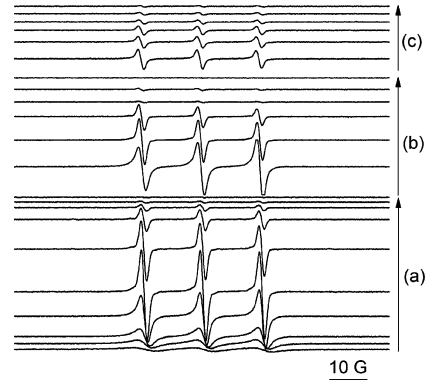

Figure 6. Deoxygenation, TEMPO decay, and regeneration in a reaction mixture containing Au/CeO_2, 3-octanol, and TEMPO (a) sealed, (b) opened to air, and resealed and (c) reopened to air and resealed, spectra each 1.2 min.

Scheme 2. Proposed Mechanism for TEMPO Acting as a Hydrogen Abstractor during the Au Catalyzed Aerobic Oxidation of Alcohols[67]

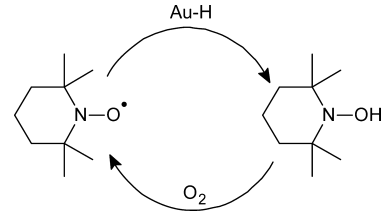

EPR spectra of $AuCeO_2$-catalyzed oxidation of 3-octanol in a sealed system in the presence of TEMPO at 80 °C are shown in Figure 6. Deoxygenation due to oxygen consumption during catalytic oxidation is observed first (line become sharper and higher in intensity). Following oxygen consumption, TEMPO decay is observed. This decay is attributed to the abstraction of a hydrogen atom from the gold surface by TEMPO leading to the formation of hydroxylamine.[65] Indeed, if the system is reopened to air and sealed again, it is possible to observe the reappearance of the TEMPO signal (due to oxidation of hydroxylamine back to TEMPO) followed by deoxygenation and a new decay (Figure 6).

This trend in TEMPO signal intensity can be rationalized if we assume two catalytic cycles with the gold catalyst abstracting a H atom from the alcohol to form Au−H, TEMPO abstracting the hydrogen from the Au surface to form hydroxylamine, and oxygen reoxidizing the hydroxylamine back to TEMPO (Scheme 2). A similar process has been proposed for Ru catalyzed oxidations.[66]

The absence of a complete regeneration of nitroxide signal is probably due to side reactions; for instance, reduction of

(57) Kohno, M.; Yamada, M.; Mitsuta, K.; Mizuta, Y.; Yoshikawa, T. *Bull. Chem. Soc. Jpn.* **1991**, *64*, 1447–1453.
(58) Rosen, G. M.; Beselman, A.; Tsai, P.; Pou, S.; Mailer, C.; Ichikawa, K.; Robinson, B. H.; Nielsen, R.; Halpern, H. J.; D.; MacKerell, A. D., Jr. *J. Org. Chem.* **2004**, *69*, 1321–1330.
(59) Connolly, T. J.; Scaiano, J. C. *Tetrahedron Lett.,* **1997**, *38*, 1133–1136.
(60) Roth, J. P.; Yoder, J. C.; Won, T.-J.; Mayer, J. M. *Science* **2001**, *294*, 2524–2526.
(61) Subczynski, W. K.; Hyde, J. S. *Biophys. J.,* **1984**, *45*, 743–748.
(62) Bobbitt, J. M.; Flores, M. C. L. *Heterocycles* **1988**, *27*, 509–533.
(63) Inokuchi, T.; Matsumoto, S.; Nishiyama, T.; Torii, S. *J. Org. Chem.* **1990**, *55*, 462–466.
(64) Zhao, M.; Li, J.; Mano, E.; Song, Z.; Tschaen, D. M.; Grabowski, E. J. J.; Reider, P. J. *J. Org. Chem.* **1999**, *64*, 2564–2566.
(65) Janiszewska, A. M.; Grzeszczuk, M. *Electroanalysis* **2004**, *16*, 1673–1681.

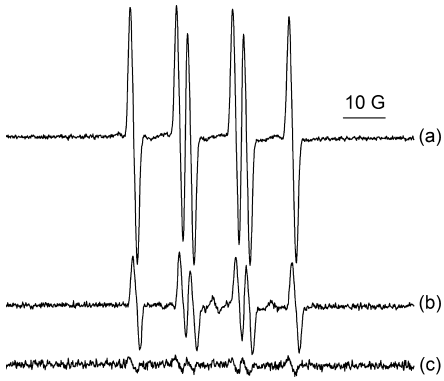

Figure 7. Oxygen-centered spin adducts over gold surface (a) Au/CeO_2, (b) CeO_2, and (c) PI-Au. Spectra were recorded at room temperature.

nitroxides often produces a small amount of amine in addition to hydroxylamine.[68]

These results place the role of oxygen in the gold-catalyzed alcohol oxidation in a new light. In a system containing an alcohol, a gold catalyst, and oxygen, the oxygen is not needed to form the final product (ketone) but is required to restore the catalytic activity by abstracting hydrogen from the gold surface. This conclusion can explain the similarities and differences in the three catalysts examined. Metal oxide supported gold catalysts provide "activated" oxygen to a high number of active sites as compared to an unsupported catalyst, thus resulting in increased activity. In contrast, unsupported gold catalysts or immobilized particles rely on the availability of oxygen in the vicinity of the gold surface, which is usually low,[69] and this quite often reduces the activity of the catalyst.

In addition, it is interesting to note that when samples of Au/CeO_2, CeO_2, or PI-Au were treated with a concentrated (1 M) DMPO solution in toluene (e.g., without any alcohol), a spin adduct with coupling constants $a_N = 13.66$, $a_H = 11.00$ G was observed, consistent with an oxygen-centered species[70] over the catalyst surface (Figure 7).

This is consistent with the ability of materials like CeO_2 to locate oxygen derived species such as superoxide, which can usually be detected at low temperature (77K) as part of the CeO_2 surface lattice.[71] The strong signals in Figure 7a, b suggest the enhanced and synergistic effect of the support as compared with the polymer immobilized catalyst.

2.5. Proposed Mechanism for Alcohol Oxidation over Gold Catalysts. The combined results of our study make it possible to propose the following overall mechanism for Au-catalyzed alcohol oxidation (Scheme 3).

Adsorption of the alcohol on the metal surface could lead to metal alkoxide (not shown in Scheme 3), which is commonly accepted as initial step during alcohol oxidation over gold surfaces.[3,72,73] Our data, however, neither prove nor disprove the formation of these species. The rate-determining step of the overall reaction is a C−H bond cleavage by the gold surface. This could occur *via* transfer of either a hydrogen atom or hydride; hydride transfer (shown in Scheme 3) is more likely according to a recent report[21] evaluating Hammet plots for the benzyl alcohol oxidation over Au/CeO_2. Formation of only a small amount of carbon and carboperoxyl radicals observed in this work is also consistent with the hydride transfer. The formation of the Au−H species could explain why gold is an excellent reduction catalyst,[74−77] although industrially relevant oxidation processes have overshadowed this reactivity. Following the C−H bond cleavage, the ketone is formed, but the catalyst surface is covered with Au−H, which must be removed to restore the catalytic activity. This is done by oxygen, leading to water, possibly *via* hydrogen peroxide through oxygen reduction reaction,[51,55] without formation of H_2. The proton released from the OH group of the alcohol is consumed during water formation. An equimolar ratio of water and ketone formed in the alcohol oxidation (*vide supra*) is consistent with the proposed mechanism.

The above mechanism is likely to be common for both supported and unsupported gold catalysts, as the H spin adduct was detected for all catalysts, and the signal intensity of this adduct showed a strong correlation with the catalyst activity. With supported catalysts, activated (i.e., coordinated) superoxide species[78] can abstract hydrogen from Au−H thus enhancing the catalytic efficiency. In the case of markedly basic metal oxides as CeO_2, formation of other adsorbed hydrogen species such as Ce−H cannot be ruled out and this could further contribute to the high activity of this catalyst, although control tests under reaction conditions did not show any presence of DMPO-H adducts when CeO_2 only was used. Formation of free peroxyl radicals consistent with an autoxidation pathway is also observed during alcohol oxidation, but it is much slower than hydride transfer; this reaction can potentially lead to side products and reduce the selectivity of oxidation.

3. Conclusion

Using supported and unsupported gold catalysts, we have demonstrated that catalytic alcohol oxidation proceeds *via* formation of a Au−H intermediate. The isotope labeling study conclusively showed that the rate determining step of the process is cleavage of the C−H bond. This process takes place *via* abstraction of hydride or a hydrogen atom from the alcohol by the gold surface. The role of O_2 in this reaction is to close the catalytic cycle (by removing the hydrogen from the gold surface), not to oxidize alcohol. The support can activate O_2, thus leading to faster recovery of the activity for the supported Au catalysts as compared to the unsupported ones. These findings can explain both the generally high selectivity of Au

(66) Dijksman, A.; Marino-González, A.; Payeras, A.; Arends, I. W. C. E.; Sheldon, R. A. *J. Am. Chem. Soc.* **2001**, *123*, 6826–6833.
(67) Control experiments show that the TEMPO-regenerated Au catalyst does not have the same initial activity. This behaviour is being further investigated.
(68) Ciriano, M. V.; Korth, H.-G.; van Scheppingen, W. B.; Mulder, P. *J. Am. Chem. Soc.* **1999**, *121*, 6375–6381.
(69) Stiehl, J. D.; Kim, T. S.; McClure, S. M.; Mullins, C. B. *J. Am. Chem. Soc.* **2004**, *126*, 1606–1607.
(70) Reszka, K.; Lown, J. W.; Chignell, C. F. *Photochem. Photobiol.* **1992**, *55*, 359–366.
(71) Martinéz-Arias, A.; Gamarra, D.; Fernandéz-García, M.; Wang, X. Q.; Hanson, J. C.; Rodriguez, J. A. *J. Catal.* **2006**, *240*, 1–7.
(72) Milone, C.; Ingoglia, R.; Pistone, A.; Neri, G.; Galvagno, S. *Catal. Lett.* **2003**, *87*, 201–209.
(73) Gong, J.; Flaherthy, D. W.; Yan, T.; Mullins, C. B. *ChemPhysChem* **2008**, *9*, 2461–2466.
(74) Claus, P. *Appl. Catal. A: Gen.* **2005**, *291*, 222–229.
(75) Lopez-Sanchez, J. A.; Lennon, D. *Appl. Catal. A: Gen.* **2005**, *291*, 230–237.
(76) Corma, A.; Serna, P.; García, H. *J. Am. Chem. Soc.* **2007**, *129*, 6358–6359.
(77) Corma, A.; Serna, P. *Science* **2006**, *313*, 332–334.
(78) Pushkarev, V. V.; Kovalchuk, V. I.; d'Itri, J. L. *J. Phys. Chem. B* **2004**, *108*, 5341–5348.

Scheme 3. Proposed Mechanism for the Au Catalyzed Aerobic Oxidation of Alcohols[a]

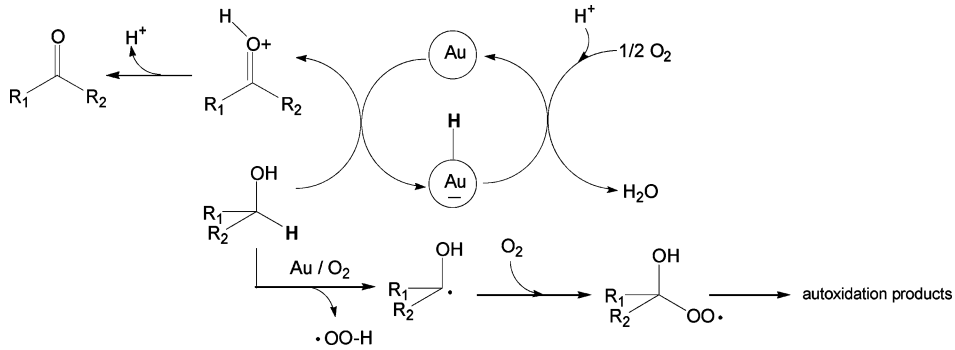

[a] Oxygen acts as a catalyst regenerator. Side products may be possible if oxygen is involved in the initial steps of the reaction (bottom) consistent the with autoxidation pathway.

based catalysts in oxidation reactions and excellent activity of Au in hydrogenation reactions.

We believe that the Au−H formation demonstrated in this work is critical for the design of highly selective Au catalysts. At the same time, the choice of a suitable support can enhance the faster recovery of catalytic activity and hence enable the catalysts to operate in milder conditions. The feasibility of forming a transient Au−H species opens up exciting possibilities for exploring other Au-catalyzed reactions.

4. Experimental Section

4.1. Chemicals. DMPO, PBN, TEMPO, and other chemicals were purchased from Aldrich and used without further purification.

Gold on nanocrystalline ceria (Au/CeO_2) was purchased from Instituto de Tecnología Química (ITQ) in Valencia and used without any further treatment. The preparation procedure for this catalyst is reported in ref 21 and references therein. The gold loading in this catalyst was 2.5 wt % with an average particle size of 4 nm and a surface area of 162 $m^2\ g^{-1}$.[34]

4.2. Preparation of Triphenylphosphine-Protected Au Nanoparticles. Triphenylphosphine-protected Au nanoparticles were synthesized by a modified biphasic method[36,79,80] and purified by gel permeation chromatography. A 1% aqueous hydrogen tetrachloroaurate trihydrate solution (5 mL) was added to a toluene solution (5 mL) of tetraoctylammonium bromide (100 mg) and stirred for 5 min. When the gold layer had transferred to the organic phase, triphenylphosphine (130 mg) was added under stirring. After 2 min, a freshly prepared aqueous solution (5 mL) of $NaBH_4$ (130 mg) was rapidly added. The organic phase immediately turned dark brown. The reaction mixture was stirred for 20 min. The toluene layer was separated, and the solvent was removed under vacuum at 40 °C to give a dark brown residue. The residue was redissolved in the minimum amount of dichloromethane and purified by gel permeation chromatography using Bio-Beads SX-1 gel (Bio-Rad) as a stationary phase and dichloromethane (Fisher) as an eluent. Yield 68%. The amount of gold in the particles (from TGA analysis) was *ca.* 76 wt%, with an average particle size of 1.4 nm (as determined by TEM).

4.3. Preparation of Polymer-Incarcerated Gold Nanoparticles. Polymer incarcerated gold nanoparticles were prepared by a modified procedure reported for Pd[81−85] and Sc[86] catalysts. Styrene based copolymer (synthesis is described in the Supporting Information) (800.0 mg) and $NaBH_4$ (10.1 mg) were dissolved in diglyme (13 mL) at room temperature. To this solution was slowly added triphenylphosphine gold(I) chloride (31.1 mg) with 3 mL of diglyme. The solution turned wine red. The mixture was stirred for 3 h at room temperature, and diethylether (30 mL) was slowly added to the mixture at room temperature. Brown coaservates enveloped the metal dispersed in the medium. The catalyst capsules were then washed with diethylether several times and dried at room temperature. Next, the catalyst capsules were heated at 150 °C for 5 h without solvent to prepare the wine red solid. The solid thus prepared was washed with dichloromethane and water, crushed, and dried to afford wine red powder. This powder was heated at 150 °C for 5 h without solvent to afford PI-Au. To determine Au composition, 20−30 mg of PI-Au were heated in a mixture of sulfuric acid and nitric acid at 200 °C for 3 h, the mixture was cooled to room temperature, and aqua regia was added. The amount of gold in the resulting solution was determined as 0.083 mmol g^{-1} by ICP analysis.

4.4. EPR Experiments. X-band EPR spectra were recorded at room temperature in deoxygenated toluene, using Jeol JES-RE1X and Bruker ESP-300E spectrometers. The typical instrument parameters were as follows: frequency 8.97 GHz, power 5 mW, sweep width 100 G, center field 3186 G, sweep time 60 s, time constant 30 ms, modulation frequency 100 kHz, modulation width 1 G, gain 200. Quantitative spectral analysis was carried out using WinSim software.[87]

The spin trapping experiments were performed as follows: 0.1 M solution of DMPO in toluene (0.2 mL) was added to the substrate (0.2 mL of neat 2-pentanol). The resultant mixture was added to a solution of gold nanoparticles (3 mg). In the case of Au/CeO_2 and PI-Au, 12 mg of catalyst were used. The mixture was transferred into a glass tube and deoxygenated by bubbling nitrogen for *ca.* 1 min before recording the EPR spectra. All experiments were carried out at 70 °C unless specified otherwise.

The amount and surface area of the catalysts and concentrations/volumes of reagents were tightly controlled and the same in all tests. We observed that the main source of experimental variability was deoxygenating and mixing of the system to have a suspension in the center of the EPR cavity. The EPR intensities were reproducible within a factor of *ca.* 2.

4.5. Bulk Catalyst Activity Test. To emulate the spin trapping reaction conditions, triphenylphosphine-protected Au nanoparticles (3 mg) were mixed with 0.5 mL of 2-pentanol at room temperature for

(79) Brust, M.; Walker, A.; Bethell, D.; Schiffrin, D. J.; Whyman, R. *J. Chem. Soc., Chem. Commun.* **1994**, 801–802.
(80) Weare, W. W.; Reed, S. M.; Warner, M. G.; Hutchison, J. E. *J. Am. Chem. Soc.* **2000**, *122*, 12890–12891.
(81) Okamoto, K.; Akiyama, R.; Kobayashi, S. *J. Org. Chem.* **2004**, *69*, 2871–2783.
(82) Okamoto, K.; Akiyama, R.; Kobayashi, S. *Org. Lett.* **2004**, *6*, 1987–1990.
(83) Miyamura, H.; Akiyama, R.; Ishida, T.; Matsubara, R.; Takeuchi, M.; Kobayashi, S. *Tetrahedron* **2005**, *61*, 12177–12185.
(84) Hagio, H.; Sugiura, M.; Kobayashi, S. *Synlett* **2005**, 813–816.
(85) Nishio, R.; Sugiura, M.; Kobayashi, S. *Org. Lett.* **2005**, *7*, 4831–4834.
(86) Takeuchi, M.; Akiyama, R.; Kobayashi, S. *J. Am. Chem. Soc.* **2005**, *127*, 13096–13097.
(87) Simulation was carried out using WinSim software: http://epr.niehs.nih.gov/pest.html.

24 h. Au/CeO_2 (100 mg) was mixed with 1.7 mL of 3-octanol and 1.7 mL of toluene at 70 °C under stirring for 14 h and under an air flow of 20 mL min^{-1}. PI-Au (100 mg) was mixed with 1.7 mL of 1-phenylethanol and 1.7 mL of toluene at 70 °C under stirring for 14 h under an air flow of 20 mL min^{-1}. The reaction mixture was dissolved in $CDCl_3$, and the conversion of starting material was determined by ^1H NMR using a Jeol ECX400 instrument operating at 400 MHz.

Acknowledgment. The authors thank EPSRC for funding (Grant EP/E001629/1). The authors would like to thank Dr. Trevor Dransfield (Centre of Excellence in Mass Spectrometry, University of York), for GC−MS determinations.

Supporting Information Available: EPR and UV−vis spectra, preparation of poly-PBN, details of styrene based copolymer synthesis, products characterization, isotope effect determination. This material is available free of charge via the Internet at http://pubs.acs.org.

JA809883C